Dispersion-Engineered and Fabrication-Robust SOI Waveguides for Ultra-Broadband DWDM

Yuyang Wang,[1],* Songli Wang,[1] Asher Novick,[1] Aneek James,[1] Robert Parsons,[1] Anthony Rizzo,[1] and Keren Bergman[1]

[1]*Department of Electrical Engineering, Columbia University, New York, NY, 10027, USA*

yw3831@columbia.edu

Abstract:　　We present a measurement-validated design methodology for engineering the width of silicon-on-insulator waveguides for co-optimized group velocity dispersion and fabrication robustness, paving the way for ultra-broadband dense wavelength-division multiplexing silicon photonic communication solutions.　© 2023 The Author(s)

1.　Introduction

Silicon photonics (SiPh) has proven a promising solution to the arising interconnect bandwidth bottleneck of data centers and high-performance computing (HPC) systems, enabling compact dense wavelength-division multiplexing (DWDM) in a complementary metal-oxide-semiconductor (CMOS)–compatible fabrication process. SiPh integrated transceivers often rely upon highly phase-sensitive devices, such as ring resonators and Mach–Zehnder interferometers (MZIs), for achieving wavelength division and signal modulation. Therefore, a fabrication-robust platform is desirable for minimizing the impact of process variations on device and link performances. While the waveguide thickness is not an accessible design parameter as it is usually specified by the foundries, the waveguide width can be engineered for better fabrication robustness [1]. With wider waveguides, phase errors due to fabrication variations is reduced because the fundamental optical mode in the waveguide becomes more contained, thus less affected by the variations of the waveguide sidewalls. The waveguide's group velocity dispersion (GVD) is also strongly dependent on it's physical dimensions, becoming an important design parameter, especially for emerging ultra-broadband DWDM applications enabled by recent advances in optical frequency comb sources and integrated optical interconnect architectures [2]. These frequency combs can provide many optical carriers with a perfectly even spacing in the frequency domain [3], requiring carefully controlled link device dispersion across a wide optical band to minimize wavelength-dependent power penalties, such as loss and crosstalk. The waveguide width must be carefully designed for an optimized trade-off between GVD and fabrication robustness, for which a validated design methodology has been lacking for silicon photonic platforms.

In this study, we propose and demonstrate a design methodology for engineering the width of silicon-on-insulator (SOI) waveguides for enabling a dispersion-minimized and fabrication-robust silicon photonic platform. Our design methodology is based on the successful development of a group index model extensively validated by both experimental measurement and simulation results. The optimal waveguide width chosen by our design methodology can achieve near-zero dispersion across the full S-, C-, and L-bands while reducing the impact of wafer-scale process variations by a factor of 2, paving the way for ultra-broadband DWDM silicon photonic communication solutions.

2.　Measurement-Validated Group Index Model

The interference fringes of MZIs can be utilized to extract the group index of constituent waveguides as $n_g = \lambda^2 / (\text{FSR} \cdot \Delta L)$, where FSR is the free spectral range defined as the wavelength spans between adjacent fringes. We measured 7 reticles, each with 135 MZIs consisting of 27 different waveguide widths (w) from 400 nm to 2500 nm and 5 different arm length delays (ΔL) from 100 nm to 500 nm, fabricated on a custom 300 mm full wafer through AIM Photonics (Fig. 1a). Devices with the same waveguide width are placed adjacently to minimize the impact of local process variations on device performance. All MZIs have a nominal waveguide height of 220 nm, and grating couplers designed for quasi-TE polarization are utilized for optical I/O. The two arms of each MZIs consist of symmetric waveguide bends to mitigate the impact of bending on the group index. For devices with waveguides beyond the single-mode cutoff width, Euler bends are used to maintain single mode operation and high mode isolation [1]. A tunable laser was swept from 1450–1610 nm at a 10 pm resolution to characterize the transmission spectrum of each MZI, with a representative spectrum shown in Fig. 1b. A subset of the extracted n_g values for 6 widths are plotted in Fig. 1c (scattered dots).
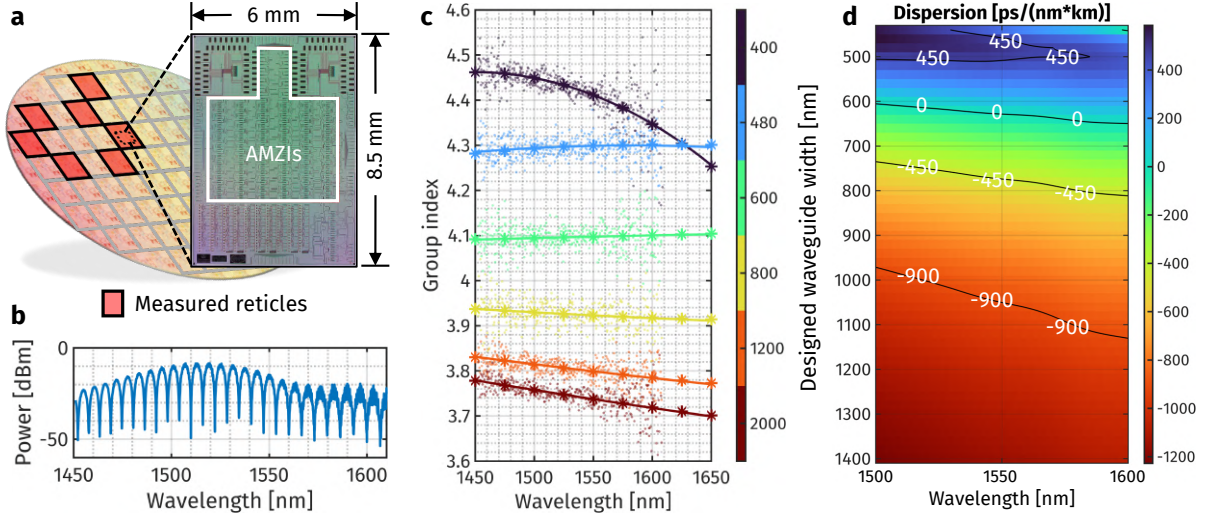
Fig. 1. **(a)** Illustration of measured reticles on a custom 300 mm wafer, with a blown-up microscopic image of a die with 135 MZIs. **(b)** Transmission spectrum of an MZI measured on reticle #2. **(c)** Our developed group index model $n_\text{g}(\lambda, w)$ (solid curves) closely matches both measured data (scattered dots) and Lumerical MODE simulation results (asterisks). **(d)** A heatmap of simulated GVD validates the $\partial n_\text{g}/\partial \lambda$ slopes observed in (c) for different waveguide widths.

We then developed an analytical model $n_\text{g}(\lambda, w)$ to describe the group index as a function of both the wavelength and the waveguide width. Based on our previously proposed effective index (n_eff) model [4], we format $n_\text{g}(\lambda, w)$ as

$$n_\text{g}(\lambda, w) = n_\text{eff}(\lambda, w) - \lambda \cdot \frac{\partial n_\text{eff}(\lambda, w)}{\partial \lambda} = \sum_{n=0}^{3} (1-n)p_n(w)\lambda^n, \quad \text{where } p_n(w) = p_{n0} \cdot \frac{w^2 + p_{n1}w + p_{n2}}{w^2 + p_{n3}w + p_{n4}}. \quad (1)$$

The choice of $p_n(w)$ as the ratio of two polynomials of equal order ensures that the group index asymptotically approaches a constant value for a given λ as w approaches infinity, corresponding to that of a slab waveguide. Considering that there is a systematic shrinkage in waveguide widths (Δw) across the fabricated wafer compared to the design values, we defined an auxiliary function

$$z(p_{nm}, \Delta w) = n_\text{g}(\lambda, w - \Delta w) - n_\text{g}^*, \quad n \in \{0, \dots, 3\}, \ m \in \{0, \dots, 4\}, \quad (2)$$

where p_{nm} denotes the fitting coefficients described in Eq. (1), and n_g^* is the extracted group index from measurement. Then, optimal p_{nm} coefficients and Δw were derived by minimizing $\sum \|z\|^2$ for all λ's and w's using a classic non-linear least squares fitting algorithm [5]. An average shrinkage of waveguide widths from design values was found to be $\Delta w = 40$ nm based on the fitting results, and the model predicted n_g values with Δw incorporated are plotted in Fig. 1c (solid curves), matching the trends of the measured data. To further validate the developed group index model, we conducted finite-difference eigenmode (FDE) simulations in Lumerical MODE for all fabricated waveguide geometries assuming $\Delta w = 40$ nm. These simulated n_g's are plotted in Fig. 1c (asterisks), showing an excellent matching with our model prediction. It is evident that $\partial n_\text{g}/\partial \lambda$ (proportional to GVD) greatly differs for different waveguide widths, for which a finer-grained relationship can be observed from the simulated dispersion heatmap in Fig. 1d.

3. Waveguide Width Engineering for Co-Optimized Dispersion and Robustness

For key components of DWDM links, like ring resonators and MZIs, fabrication variations of waveguide dimensions can result in FSR deviations (ΔFSR) and resonance shifts ($\Delta\lambda$) from their design values, both of which need to be managed in ultra-broadband applications. In Fig. 2a, using our proposed analytical model, we extracted the group index of each measured MZI and observed its standard deviation (σ_{n_g}) at 1550 nm as a function of the waveguide width (Fig. 2b). Smaller variation magnitudes of measured n_g at larger widths indicate improved fabrication robustness of wider waveguides. Compared to FSR variations governed by ΔFSR $\approx (\Delta n_\text{g}/n_\text{g}) \cdot \lambda \cdot (\lambda_\text{res}/L)$, the resonance wavelength variations, governed by $\Delta\lambda = (\Delta n_\text{eff}/n_\text{g}) \cdot \lambda$, is more sensitive to the change in n_eff due to the lack of the L term in the denominator, defined as the interferometric path length.

Therefore, we study the trade-off between $\partial n_\text{eff}/\partial w$ (blue, indicating fabrication robustness) and $\partial n_\text{g}/\partial \lambda$ (red, proportional to dispersion) by plotting both in Fig. 2c. Both $\partial n_\text{eff}/\partial w$ and $\partial n_\text{g}/\partial \lambda$ were derived from our proposed
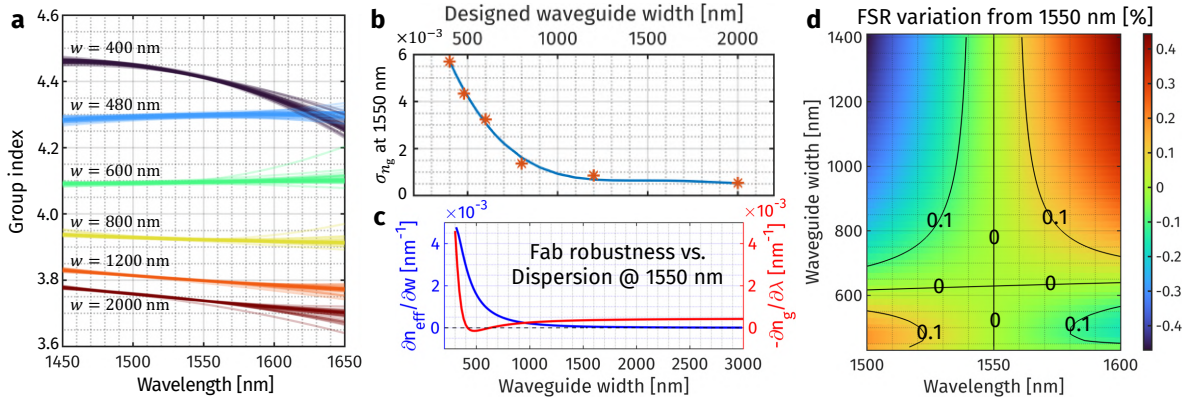
Fig. 2. **(a)** Extracted group indices from experimental measurements at six selected widths. 35 devices are measured at each width. **(b)** Calculated σ_{n_g} at 1550 nm for the 6 device widths (asterisks) as well as a fit curve, confirming measured reduction in fabrication variation as a function of waveguide width. **(c)** Fabrication robustness and dispersion plotted against waveguide width as calculated by the proposed model, in good agreement with our measured results. **(d)** A heatmap of the normalized FSR variation of an MZI targeting a specific FSR at 1550 nm. For $w = 630$ nm, we can expect negligible FSR variation across the S-, C-, and L-bands.

group index model, and are in good agreement with experimental measurements. From the plot, we found 630 nm to be the approximately zero dispersion width at 1550 nm. This is again validated by the measurement results in Fig. 1c. A $\approx 53\%$ improvement in $\partial n_{\mathrm{eff}}/\partial w$ is observed if adopting 630 nm waveguides, compared to the 480 nm waveguides provided by the foundry process design kit (PDK). Further improving the fabrication robustness by choosing larger widths requires investigation of dispersion impact on the FSR. We thus derived an FSR variation heat map (Fig. 2d) showing the normalized deviation of the FSR from that of 1550 nm for various waveguide widths. The heat map shows that with 800 nm waveguides, the FSR deviation can be restricted within 0.1 % for ring resonators or MZIs over the full C-band, 1525 nm to 1575 nm, capable of supporting dozens of DWDM channels, while also achieving $\approx 78\%$ improvement in fabrication robustness. For applications where fabrication robustness is more critical than minimizing ultra-broadband dispersion, $\geqslant 800\%$ improvement in fabrication robustness is possible with wider waveguides ($w > 1200$ nm).

4. Conclusion

We presented a design methodology for engineering the width of SOI waveguides for achieving co-optimized group velocity dispersion and fabrication robustness on CMOS-compatible silicon photonic platforms. Based on our group index model extensively validated by both measurement and simulation, the optimal waveguide width chosen by our design methodology can achieve near-zero dispersion across the full S-, C-, and L-bands, while improving fabrication robustness by $2\times$. For less dispersion sensitive applications, our design methodology can also target design points with almost an order of magnitude improved fabrication robustness.

References

1. A. Rizzo, U. Dave, A. Freitas, S. P. Roberts, A. Novick *et al.*, "Fabrication-robust silicon photonics platform in standard 220 nm silicon processes," in *2021 IEEE 17th International Conference on Group IV Photonics (GFP),* (2021), pp. 1–2.
2. A. Rizzo, S. Daudlin, A. Novick, A. James *et al.*, "Petabit-scale silicon photonic interconnects with integrated kerr frequency combs," IEEE J. Sel. Top. Quantum Electron. **29**, 1–20 (2023).
3. B. Y. Kim, Y. Okawachi, J. K. Jang *et al.*, "Turn-key, high-efficiency kerr comb source," Opt. Lett. **44**, 4475–4478 (2019).
4. A. James, Y. Wang, A. Rizzo, and K. Bergman, "Flexible, process-aware compact model of effective index in silicon waveguides for commercial foundries," in *2022 International Conference on Numerical Simulation of Optoelectronic Devices (NUSOD),* (2022), pp. 173–174.
5. T. F. Coleman and Y. Li, "An interior trust region approach for nonlinear minimization subject to bounds," SIAM J. on Optim. **6**, 418–445 (1996).